

Structural Variation in the $Y_{3-c}Pr_cScFe_4O_{12}$ Garnet System

P. D. DERNIER, E. M. GYORGY AND W. H. GRODKIEWICZ

Bell Laboratories, Murray Hill, New Jersey 07974

Received August 20, 1973

Structural refinements from single crystal X-ray diffraction data of four members of the garnet series, $Y_{3-c}Pr_cScFe_4O_{12}$, have revealed a nonlinear variation in oxygen positional coordinates versus Pr concentration. As a result of this anomaly the various polyhedra in the cubic unit cell expand and contract in an interdependent fashion such that the lattice parameter, a_0 , varies nearly linearly with concentration. This finding is related to recent magnetic anisotropy measurements as well as the crystal chemistry of the garnets in general.

Introduction

Recent magnetic studies of the $Y_{3-c}Pr_cScFe_4O_{12}$ series have revealed a highly nonlinear variation in the anisotropy constant K_1 versus Pr concentration and lattice constant (l). In order to explain this behavior it has been proposed that changes in the internal structure of the unit cell, specifically the variation in size and distortion of the rare-earth polyhedron, may be more directly correlated with this property. In addition, the concept of anomalous variation in structure despite linear unit cell expansion is of general interest from the crystal chemical point of view. In order to test these concepts it was necessary to refine the structures of four members of the series from single crystal X-ray intensity data. In this paper we report the results of these structural refinements and relate them to the above mentioned problems.

Experimental

Crystals of the series $Y_{3-c}Pr_cScFe_4O_{12}$ were grown from a $PbO-PbF_2-B_2O_3$ flux by standard methods (2, 3). Crystals of Y_1Pr_2

$ScFe_4O_{12}$, for example, weighing up to 12 g were grown from the following melt:

Crystal component	g	Flux component	g
Y_2O_3	14.1	PbO	120
Pr_2O_3	41.2	PbF ₂	146
Sc_2O_3	10.3	B_2O_3	6.6
Fe_2O_3	48.0	CaO	0.284

The components were melted together in a covered 100 ml. platinum crucible in a Harper muffle furnace and cooled from 1250°C to 1000°C at $\sim \frac{3}{4}$ °C per hour while blowing oxygen through the furnace. The flux was poured from the crucible at the lower temperature. The nominal formulas for the four members of the series considered for study were $Y_{2.97}Pr_{0.03}ScFe_4O_{12}$, $Y_2PrScFe_4O_{12}$, $YPr_2ScFe_4O_{12}$, and $Pr_3ScFe_4O_{12}$. For the first member, a comparison of lattice parameter with that reported earlier by Geller (4) indicated that the actual scandium content was somewhat less. Therefore, atomic absorption analysis was performed on the remaining

members of the series in order to obtain more realistic estimates of the Sc/Fe ratio. In addition the Y/Pr ratio for the intermediate members was refined together with the atomic positional parameters from single crystal X-ray intensity data. The actual compositions which are believed to be accurate to $\pm 3\%$ for Sc and Fe and $\pm 5\%$ for Y and Pr are as follows.

Sample No.	Composition	Lattice constant (Å)
1	$Y_{2.97}Pr_{0.03}Sc_{0.8}Fe_{4.2}O_{12}$	12.439
2	$Y_{2.3}Pr_{0.7}Sc_{0.8}Fe_{4.2}O_{12}$	12.518
3	$Y_{1.0}Pr_{2.0}Sc_{0.97}Fe_{4.03}O_{12}$	12.639
4	$Pr_3Sc_{0.94}Fe_{4.06}O_{12}$	12.737

The lattice constants were determined by a simplified version of Bond's method (5, 6) for each individual crystal later used in X-ray intensity data collection.

Single crystal intensity measurements were taken with a paper tape controlled GE XRD-5 X-ray diffractometer. The radiation used was $MoK\alpha$ with Zr filter. An 8° take-off angle was used along with a scintillation counter as detector. Each specimen was ground into a sphere, oriented and all independent reflections within $\frac{1}{8}$ of the sphere of reflection with $80^\circ \geq 2\theta \geq 25^\circ$ were measured. The integrated intensities were collected by the

stationary-crystal stationary-counter technique. The background was measured $\pm 2^\circ$ of 2θ off each peak maximum, averaged and then later subtracted from the peak intensity to yield a net value. The intensity of a general reflection typically represented an average of six measurements taken from six different planes of the same crystallographic form. Pertinent data for each crystal specimen along with the linear absorption coefficients, μR , are as follows.

Sample No.	Radius (mm)	μR	ϕ axis	Number of independent reflections
1	0.145	3.656	[001]	104
2	0.158	3.714	[110]	134
3	0.171	3.713	[001]	226
4	0.189	3.803	[001]	256

Those reflections for which the peak intensity was not at least twice the background were considered unobserved.

Refinement

For each structural refinement the starting positional parameters were those reported by Geller for $Y_3Fe_5O_{12}$ (7). The atomic form factors for neutral Y, Pr, Sc, Fe, and O given by Cromer and Waber were used along

TABLE I
 $Y_{3-c}Pr_cScFe_4O_{12}$ FINAL PARAMETERS

<i>c</i>	0.03	0.70	2.0	3.0
Scale factor	0.180(2)	0.208(2)	0.246(2)	0.287(3)
Sec. Ext. coefficient	0.00014(5)	0.00022(4)	0.00016(2)	0.00017(3)
<i>B</i> (Y, Pr)	0.22(4)	0.31(4)	0.48(3)	0.50(2)
<i>B</i> (Sc, Fe)	0.43(4)	0.57(5)	0.57(6)	0.62(7)
<i>B</i> (Fe)	0.47(6)	0.39(3)	0.45(3)	0.43(4)
Oxygen— <i>x</i>	0.9728(6)	0.9738(4)	0.9717(3)	0.9710(4)
Oxygen— <i>y</i>	0.0575(6)	0.0565(4)	0.0545(3)	0.0545(4)
Oxygen— <i>z</i>	0.1515(6)	0.1517(5)	0.1521(3)	0.1513(4)
<i>B</i> (O)	0.50(10)	0.84(10)	1.05(6)	0.78(6)
<i>R</i>	0.022	0.025	0.027	0.031
<i>wR</i>	0.037	0.039	0.051	0.055

TABLE II
INTERATOMIC DISTANCES AND BOND ANGLES^a

<i>c</i>	0.03	0.70	2.0	3.0
Rare-earth polyhedron				
RE-O(1) × 4	2.441(7) Å	2.468(5) Å	2.521(4) Å	2.539(5) Å
RE-O(2) × 4	2.365(7)	2.365(6)	2.399(4)	2.430(5)
O(1)-O(4) × 4	2.777(16)	2.793(11)	2.875(9)	2.971(9)
O(1)-O(2) × 4	2.724(14)	2.730(9)	2.796(8)	2.815(8)
O(1)-O(7) × 2	2.982(14)	3.037(10)	3.067(9)	3.074(9)
O(2)-O(6) × 2	2.836(16)	2.837(11)	2.831(9)	2.872(9)
O(1)-O(3) × 2	3.921(15)	3.948(10)	4.059(9)	4.098(9)
O(2)-O(4) × 2	3.855(15)	3.857(11)	3.951(9)	4.002(9)
Octahedron				
(Sc, Fe)-O(1) × 6	2.044(9)	2.053(6)	2.073(5)	2.081(5)
O(1)-O(2) × 6	2.724(14)	2.730(9)	2.796(8)	2.815(8)
O(1)-O(9) × 6	3.048(15)	3.067(10)	3.062(8)	3.067(8)
Tetrahedron				
Fe-O(7) × 4	1.868(8)	1.882(6)	1.871(4)	1.886(5)
O(7)-O(9) × 4	3.153(14)	3.185(9)	3.160(8)	3.180(8)
O(7)-O(14) × 2	2.836(16)	2.837(11)	2.831(9)	2.872(9)
(Sc, Fe)-Fe	3.477	3.499	3.533	3.560
(Sc, Fe)-RE	3.477	3.499	3.533	3.560
Fe-RE	3.110	3.130	3.159	3.184
Fe-RE	3.808	3.833	3.870	3.900
Angles				
(Sc, Fe)-O(9)-Fe	125.3°	125.5°	127.1°	127.5°
(Sc, Fe)-O(1)-RE	101.3	101.0	100.1	100.3
(Sc, Fe)-O(2)-RE	103.8	104.5	104.1	103.9
Fe-O(7)-RE	123.7	123.0	122.9	122.9
Fe-O(4)-RE	93.8	94.2	94.7	94.2
RE-O(2)-RE	104.8	104.9	103.7	103.4

^a The numbers in parentheses such as 2.441(7) Å are to be read 2.441 ± 0.007 Å.

with the anomalous dispersion coefficients $\Delta f'$ and $\Delta f''$ reported by Cromer in a least squares refinement program written by Prewitt (8, 9, 10). Convergence was reached after the first few cycles of refinement where the scale factor, secondary extinction coefficient, rare-earth ratio (samples 2 and 3 only), four isotropic temperature factors, and three oxygen coordinates were varied. Anisotropic thermal parameters were not introduced in the final cycles of refinement, since isotropic motion was previously determined to be a good approximation (11). A list of observed and calculated structure factors is available upon request. The final positional parameters, thermal coefficients, B , conven-

tional R ,* and wR † factors are reported in Table I. These values together with the lattice parameters were used as input to the program ORFEE (12) which calculated interatomic distances and bond angles reported in Table II.

Discussion

The $Y_{3-c}Pr_cScFe_4O_{12}$ garnet structures are cubic, space group $Ia\bar{3}d$, with eight formulas per unit cell. The cations are all in special

* $R = \sum |F_o - F_c| / \sum |F_o|$, where F_o and F_c are the observed and calculated structure factors, respectively.

† $wR = [\sum w(F_o - F_c)^2]^{1/2} / (\sum wF_o^2)^{1/2}$, where $w = (1/0.05)F_o$ for all $F_o \geq 20$ and $w = 1.0$ for all $F_o < 20$.

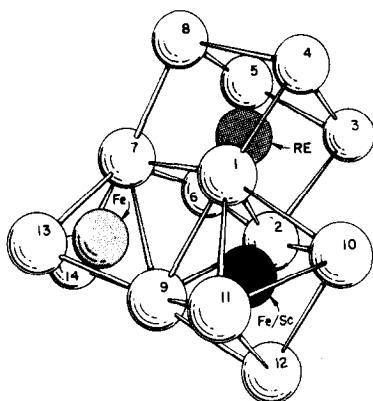


FIG. 1. A portion of the $Y_{3-c}PrScFe_4O_{12}$ garnet structure is shown with each type of polyhedron depicted. The Y and Pr ions, labeled RE, are in eightfold sites in the form of a distorted cube. The Sc and some of the Fe ions, labeled Fe/Sc, are in octahedral configuration with the remaining Fe ions in the tetrahedral configuration.

positions with yttrium and praseodymium in eightfold coordination in sites $24(c)-(0, \frac{1}{4}, \frac{1}{8})$, scandium and iron in octahedral sites $16(a)-(0, 0, 0)$, and the remaining iron atoms in tetrahedral coordination in sites $24(d)-(0, \frac{1}{4}, \frac{3}{8})$. The 96 oxygen anions are in

general position $96(h)-(x, y, z)$ with four nearest neighbors, two cations in $24(c)$ sites and one each in $16(a)$ and $24(d)$ sites. The possibility of some other type of cation disorder seems unlikely and may be reasonably rejected on ionic size considerations.

From Fig. 1 and Tables I and II one can immediately see that the three oxygen coordinates uniquely determine the size and shape of all the polyhedra. Hence the variation in distortion of these polyhedra across the series must be interdependent in some fashion. If the coordinates of oxygen remained nearly constant then each polyhedron would expand uniformly as the lattice parameter in Fig. 2. However, the octahedron and especially the tetrahedron have constrained dimensions and, therefore, the oxygen x and y coordinates vary significantly between the second and third members of the series resulting in the rather erratic cation-anion distances plotted in Fig. 3. If one takes the maximum variation in these distances as an indication of flexibility then the iron tetrahedron appears rather rigid with a maximum variation of ≈ 0.02 Å in Fe-O separation. The octahedron is less rigid with a variation of 0.04 Å across the series. [It should be noted that the change in Sc/Fe ratio for the second and third members could produce only an 0.01 Å expansion in

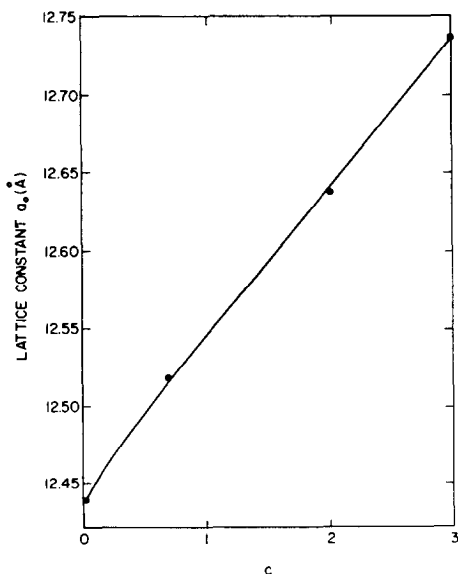


FIG. 2. The lattice constant, a_0 , of the series $Y_{3-c}PrScFe_4O_{12}$ is plotted versus Pr concentration.

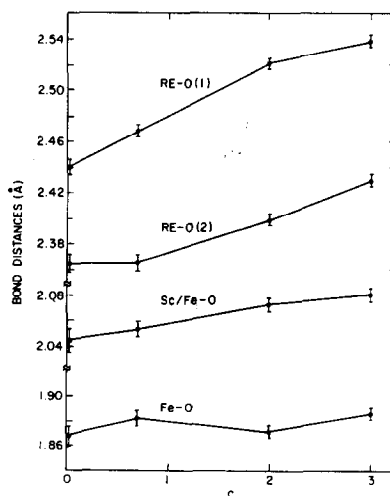


FIG. 3. Bond distances for the various polyhedra are plotted against Pr content.

the (Sc, Fe)-O distance based on size effects alone.] Finally the rare-earth polyhedron is most flexible with a variation in the average (Y,Pr)-O distance of 0.08 Å. However, the difference in radii between eight coordinated Y^{3+} and Pr^{3+} is considerably more than this latter variation, ≈ 0.125 Å, according to the effective ionic radii reported by Shannon and Prewitt (13). It is clear that the average (Y,Pr)-O distance becomes progressively smaller than the predicted distance as one proceeds across the series. The pairs of observed and calculated values for the individual members are 2.403–2.395, 2.417–2.424, 2.460–2.480, and 2.484–2.520 Å, respectively. The rare-earth polyhedron which shares two edges with adjacent tetrahedra and three edges with adjacent octahedra has been limited in its expansion. Conversely from the pairs of observed and calculated (Sc,Fe)-O distances 2.044–2.065, 2.053–2.065, 2.073–2.075, and 2.081–2.075 Å it appears that the octahedron is initially compressed and expands to a slightly larger size than predicted. The tetrahedron oscillates slightly in size as seen from the respective pairs of observed and calculated Fe-O separations of 1.868–1.870, 1.882–1.870, 1.871–1.870, and 1.886–1.870 Å.

Magnetic anisotropy measurements of the entire $Y_{3-c}Pr_cScFe_4O_{12}$ series appear to be more strongly correlated with these internal structural changes than the rare-earth concentration. As seen from Fig. 4 where the anisotropy constant K_1/Pr is plotted against Pr concentration a highly nonlinear behavior is evident (1). Clearly there are two distinct regions which qualitatively follow the bond

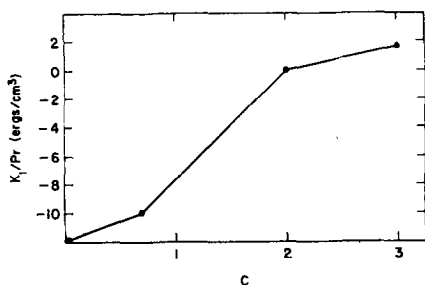


FIG. 4. The magnetic anisotropy constant K_1 per Pr ion is plotted versus Pr concentration for the $Y_{3-c}Pr_cScFe_4O_{12}$ series.

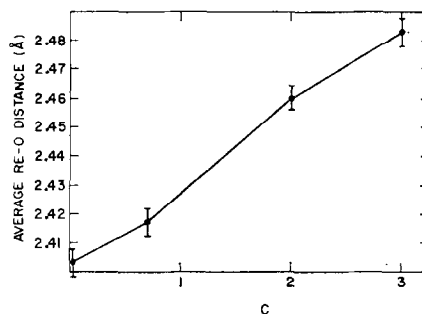


FIG. 5. The average rare earth, RE, oxygen separation is plotted against Pr concentration for the four members of the garnet series.

length and angle variations of the rare-earth polyhedron, such as the average (Y,Pr)-O distance (Fig. 5). Certain O-O separations and the Re-O-RE angle (see Table II), also follow this pattern. Although it is not possible to propose a quantitative relationship between K_1/Pr and these structural variables, it is nevertheless important to note their strong correlation.

The garnet series $Y_3Al_{5-x}Ga_xO_{12}$ provides another example of this nonlinear type of polyhedron distortion versus concentration. In this series the gallium ion can enter two possible sites, either the tetrahedral or octahedral. Previous structural refinements of four members of this series from single crystal X-ray data have yielded the cation distribution and oxygen positional parameters (11). If one plots the (Al,Ga)-O distances of the octahedron and tetrahedron versus Ga concentration in the respective sites severe deviations from linearity occur. The expansions are negatively correlated such that when the tetrahedron expands most, the octahedron expands least and vice versa, while the average Y-O distance remains nearly constant.

Conclusion

In the context of the previous discussion one may propose that the $Y_{3-c}Pr_cScFe_4O_{12}$ and $Y_3Al_{5-x}Ga_xO_{12}$ series are not particularly unique but rather are representative examples of very general types of structural variation

with changing composition. That is, substitution of cations with different ionic radii (or site preference) in selected sites will by the nature of the crystal symmetry effect the distortion of surrounding polyhedra in some compensating fashion. The net effect is a nearly linear expansion in lattice constant which completely masks the irregular behavior in the internal distortion of the unit cell. This latter concept is rather important from the point of view of incremental changes in composition and lattice parameter producing so-called "anomalous" changes in physical variables. It would appear likely that re-evaluation of these measurements in terms of structural changes would prove valuable.

Acknowledgments

We thank R. L. Barns and A. S. Cooper for their precise measurement of the garnet lattice parameters and W. M. Walsh, Jr., M. Marezio and D. B. McWhan for their interest and support. We also thank J. P. Remeika and J. M. Voorhoeve for many helpful discussions concerning this work.

References

1. E. M. GYORGY, R. C. LECRAW, A. ROSENCHWAIG, L. G. VAN UITERT, R. D. PIERCE, R. L. BARNES, AND E. HEILNER, *Phys. Rev. B* **8**, 279 (1973).
2. L. G. VAN UITERT, W. H. GRODKIEWICZ, AND E. F. DEARBORN, *J. Amer. Ceramic. Soc.* **48**, 105 (1965).
3. W. H. GRODKIEWICZ, E. F. DEARBORN, AND L. G. VAN UITERT, in "Crystal Growth" (H. S. Peiser, Ed.), p. 441. Pergamon, New York (1967).
4. W. H. VON AULOCK, "Handbook of Microwave Ferrite Materials," Academic Press, New York (1965).
5. W. L. BOND, *Acta. Cryst.* **13**, 814 (1960).
6. R. L. BARNES, *Mater. Res. Bull.* **2**, 273 (1967).
7. S. GELLER AND M. A. GILLES, *J. Phys. Chem. Solids* **3**, 30 (1957).
8. D. T. CROMER AND J. T. WABER, *Acta Cryst.* **18**, 104 (1965).
9. D. T. CROMER, *Acta Cryst.* **18**, 17 (1965).
10. C. T. PREWITT (unpublished least-squares refinement program).
11. M. MAREZIO, J. P. REMEIKA, AND P. D. DERNIER, *Acta Cryst.* **B24**, 1670 (1968).
12. W. R. BUSING AND H. A. LEVY, ORNL Report No. 59-12-3 (1959).
13. R. D. SHANNON AND C. T. PREWITT, *Acta Cryst.* **B25**, 925 (1969).